Thin Solid Films 519 (2011) 6246–6251

Contents lists available at ScienceDirect

Thin Solid Films

journal homepage: www.elsevier.com/locate/tsf

Microstructure, mechanical and tribological properties of Ti(C, N)/a-C gradient composite films

Bin Li [a], Guojun Zhang [a,b,*], Peng Zhang [a], Gang Liu [a]

[a] State Key Laboratory for Mechanical Behavior of Materials and School of Materials Science and Engineering, Xi'an Jiaotong University, Xi'an 710049, PR China
[b] School of Materials Science and Engineering, Xi'an University of Technology, Xi'an 710048, PR China

ARTICLE INFO

Article history:
Received 1 June 2010
Received in revised form 28 March 2011
Accepted 29 March 2011
Available online 6 April 2011

Keywords:
Multilayers
Nanocomposites
Wear resistance
Ti(C, N)/a-C
Transmission electron microscopy
Sputtering

ABSTRACT

Ti(C, N)/a-C composite films with compositional gradient from Ti–TiN–Ti(C, N) to Ti-containing a-C layers have been prepared by closed-field unbalanced magnetron sputtering. Within the composite films, the carbon contents gradually increase and achieve maximum in the a-C layer by increasing the power applied to the graphite targets, the nitrogen contents gradually decrease to zero from Ti(C, N) layer of the interface to a-C layer of the films. In order to achieve a good combination of the mechanical and tribological properties in the composite films, a designed experimental parameter basing on various substrate rotation speeds is also selected. Results show that the compositional gradient result in the microstructure change of composite films where the Ti(C, N) layers consist of fine nanocolumnar Ti(C, N) grains and the a-C layers consist of 2–7 nm TiC nanocrystallites embedded in an amorphous C matrix. The Ti(C, N) layers also exhibit clear multilayer structure where the period thickness gradually decreases as substrate rotation speed increases. Under higher rotation speed, disappearance of the multilayer structure is accompanied with simultaneous increase in the crystallinity of Ti(C, N) layer and also the Ti(C, N) grain size. In the a-C layer, the TiC nanocrystallites embedded in the a-C matrix is produced by the high rotation speeds. The Ti(C, N)/a-C gradient composite films exhibit high microhardness values (~5000 H_V) and low friction coefficient (~0.15), which is related to the hard Ti(C, N) layer and self-lubricate a-C layer, respectively. The combination of the Ti(C, N) layer with a-C layer increases the load and the wear resistance capacity of the composite films, which gives satisfactory friction performance in the pin-on-disk tests with a wear rate of 3.7×10^{-17} m^3/mN.

1. Introduction

Due to their high hardness and good thermal stability, Ti(C, N) films are well suitable for application in machining tools to increase the performance. However, the friction coefficient of the films is unfavorably high at room temperature [1]. Although the friction coefficient of the Ti(C, N) films can be somewhat decreased by adjusting the composition, such as raising the carbon content, the decreasing effect is limited because it is usually achieved at the expense of decrease of hardness of films [2–4]. On the other hand, it is known that the amorphous carbon films possess attractive tribological properties, such as low friction coefficient combined with high wear resistance [5]. But the magnetron sputtered carbon films are characterized by high intrinsic stresses, which make them easily delaminate even at very thin thickness and therefore restrict their applications in cutting industry. Alternately, Ti-containing amorphous carbon films (TiC/a-C), deposited by magnetron sputtering using a gradient films such as Ti–TiC and Ti–Ti(C, N), can improve adhesion and simultaneously decrease intrinsic stress [6]. However, this single layer TiC/a-C film is not enough to meet the ever-increasing demand in various tribological situations, especially in high speed and dry cutting applications where high strength and self-lubrication are needed [7]. More advanced composite films are thus urgently required.

In this paper, Ti(C, N)/a-C gradient films are deposited by closed-field unbalanced magnetron sputtering ion plating, which combines superior friction properties of the Ti-containing a-C films and the high hardness of Ti(C, N) films. The effects of the rotation speed (RS) of substrate on the nanostructure and properties of gradient films are investigated. The comprehensive properties of this kind of films can be optionally adjusted to obtain an optimization in the friction and mechanical properties, which can make the films have more extensive applications.

2. Experiments

Ti(C, N)/a-C gradient composite films were deposited respectively on high-speed steel for measurements of mechanical and tribological properties and on single crystal Si for microstructure analysis by closed-

* Corresponding author at: State Key Laboratory for Mechanical Behavior of Materials and School of Materials Science and Engineering, Xi'an Jiaotong University, Xi'an 710049, PR China. Tel.: +86 29 8231 2592; fax: +86 29 8231 2994.
E-mail address: zhangguojun@mail.xjtu.edu.cn (G. Zhang).

0040-6090/$ – see front matter © 2011 Elsevier B.V. All rights reserved.
doi:10.1016/j.tsf.2011.03.117

field unbalanced magnetron sputtering ion plating system (CFUBMSIP system). The deposition system (UDP450, Teer Coating Limited) is a cylindrical PVD reactor with four unbalanced magnetrons where two titanium targets and two graphite targets were settled opposite to each other that vertically surround the rotating substrate holder. Adjacent magnetrons have opposite magnetic polarities and the field lines are a closed field configuration. The CFUBMSIP system had been described elsewhere [8,9]. The substrates of high-speed steel and single crystal Si were placed on the substrate holder and rotated around the chamber axis with different rotation speeds. The substrates were sputter-cleaned in an Ar atmosphere. Subsequently, a Ti adhesion layer was deposited to improve the interfacial adhesion, which was followed by a TiN layer. During the deposition of Ti(C, N) layer, C targets and Ti targets were alternately sputtered by using Ar^+ and. At the same time, N_2 was continuously introduced into the chamber. The discharge gas Ar_2 with a constant flow rate was settled at 15 Sccm and the reacting gas N_2 was controlled by a built-in closed-loop optical emission monitor (OEM) through regulating the reactivity of Ti^+ with the OEM settling point at 60% for deposition of Ti(C, N) layer. Subsequently, the current of graphite targets were increased and the current of titanium targets were decreased to a fixed value for the deposition of a-C composite layer. In the stage of a-C composite layer, the Ar_2 with a constant flow rate was settled at 8 Sccm. Before deposition, a base pressure of 4×10^{-3} Pa was reached, the substrates were then plasma etched in Argon for 10 min. Subsequently, Ti(C, N)/a-C gradient films were deposited using different substrate rotation speeds of 3 rpm, 5 rpm and 8 rpm, respectively. The temperature of substrates, detected by an infrared radiation thermometer, was lower than 600 K during all deposition. No intentional heating was applied and all films were deposited at a DC pulsed bias voltage of −50 V and frequency of 50 kHz during the deposition stage of composite films. For each film, the deposition time was fixed as 120 min.

After deposition, crystalline phases of the thin films on the single crystal Si substrates were characterized by X-ray diffraction (XRD) using a XRD-7000S Diffractometer in the θ–2θ configuration which used Cu Kα radiation and operated at 40 kV. The cross-sectional microstructure of Ti(C, N) layer and a-C layer in the Ti–TiN–Ti(C, N)/a-C gradient composite films were analyzed by transmission electron microscopy (TEM, JEOL JEM-3010) operated at 300 kV. High-resolution TEM (HRTEM) was also used to study detailed microstructure of the a-C layer. Representative parts of the films on Si substrates for TEM analysis were cut for 2×2 mm size as a cross-section and two film samples were bonded together, carefully ground to proper thickness approximately hundreds of microns, polished and adhered with copper ring in the smooth cross-section and again ground in the opposite side to tens of microns, polished and thinned by FISCHIONE 1010 ion mill using an ion beam to electron transparency. Measurements on the microhardness of high-speed steel-supported films were performed on a Tukon 2100 B microhardness tester using a Vickers diamond indenter and applying a 100 gf load for the high-speed steel substrate and a 20 gf load for the films with a force hold-time of 10 s. At least 8 measurements were made for each sample and the indent morphologies were observed by SEM to evaluate the composite hardness values. To prevent the effects of substrate and film thickness on the film hardness, the intrinsic hardness of the film was calculated based on the empirical model given by Jonsson and Hogmark [10]. Friction coefficients of the films on the high-speed steel substrates were measured by a pin-on-disk tribometer using WC as sliding counterpart. The sliding speed was selected as 200 mm/s and the load was fixed as 6 N. The specific wear rate was also calculated and the features of the wear traces were observed by an optical microscope.

3. Results

3.1. Microstructure analysis

At different substrate rotation speeds, the crystalline phases comprised in the composite films have been evaluated by XRD, as shown in Fig. 1. It is found that the composite films mainly contain B1-NaCl type $TiC_{0.7}N_{0.3}$ crystalline phase, a Ti(C, N) solid solution caused by the entrance of C atoms into the TiN lattice during deposition. Besides the $TiC_{0.7}N_{0.3}$ phase, a small quantity of TiC phase can be also observed, which suggests that a few Ti atoms have entered into the a-C layer. No observation of the carbon peaks indicates the amorphous state for surface C layers. These results are in agreement with the previous reports [5,11]. The rotation speed of the substrates has slight effect on the type of formed phases but the peaks become broader and their intensities become weaker with the decrease in the rotation speeds, showing gradually reduced grain sizes.

Fig. 2 shows the cross-view TEM images of Ti(C, N) layer from the Ti(C, N)/a-C films and its corresponding selected area electron diffraction (SAED) patterns. The Ti(C, N) layers exhibit a dense columnar structure with fine nanograins. The average column diameter is below 15 nm, as shown in Fig. 2(b). From Fig. 2(a) and (b), a clear multilayer structure can also be observed in the Ti(C, N) layers and measurements show the period thicknesses of the multilayer Ti(C, N) layers are 2.0 nm and 1.8 nm, respectively, under RS of 3 rpm and 5 rpm. Increasing the RS, the multilayer structures of the Ti(C, N) layers are gradually refined until they even disappeared while the crystallinity of the Ti(C, N) layers increases, which can be seen from the corresponding SAED pattern of Fig. 2. Together with the appearance of the multilayer structure and the increase of the period thicknesses, an obvious evolution from nanocolumnar microstructure to dense nanocrystallite have arisen, accompanying with the decrease in grain size. The refinement of microstructure of Ti(C, N) layers suggests that the columnar growth of Ti(C, N) is suppressed by the multilayer structure of layer. The effect is strongly sensitive to the period thicknesses of the films as shown in Fig. 2. It is noted that the partial discontinuous column boundaries is observed from the films deposited by the low rotation speed in Fig. 2(a). In fact, the results also appear in the corresponding a-C layer as illustrated by the TEM of a-C layer below.

Fig. 3 shows the cross-view TEM images of a-C layer from the Ti(C, N)/a-C gradient films and its corresponding selected area electron diffraction (SAED) patterns. The a-C films show typical nanocomposite structure according to the results of TEM observation and corresponding SAED patterns. In Fig. 3(a), fine nanograins are determined as TiC from the XRD as well as SAED results, which are dispersed in the amorphous C matrix. There are not visible grains found in the C matrix from Fig. 3(b) and Fig. 3(c). It is suggested that the TiC nanograins with finer size distributed in the a-C matrix. Different from the Ti(C, N) layer, the surface a-C layers have not appeared in the multilayer structure even though the layers are deposited by the lower rotation speed such as 3 rpm. From Fig. 3(a), partial columnar growth pattern with discontinuous and weak column boundaries is also observed in the local region of a-C layers but

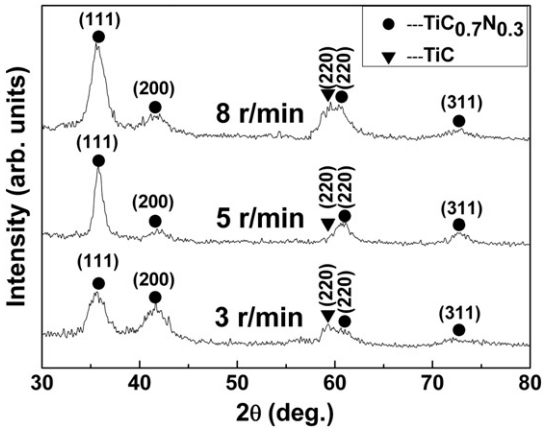

Fig. 1. XRD patterns of Ti(C, N)/a-C gradient films deposited by different rotation speeds of substrate.

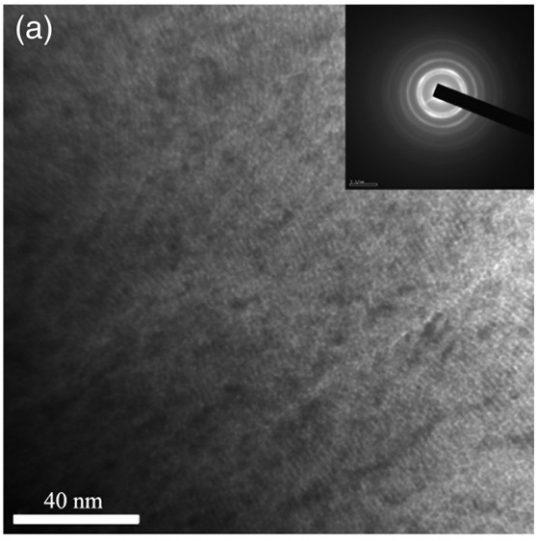

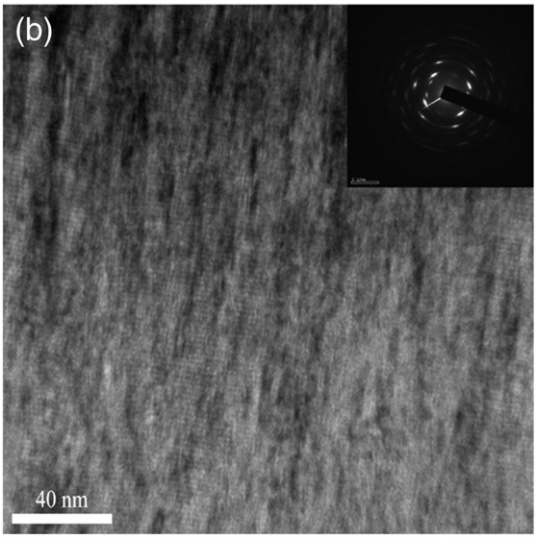

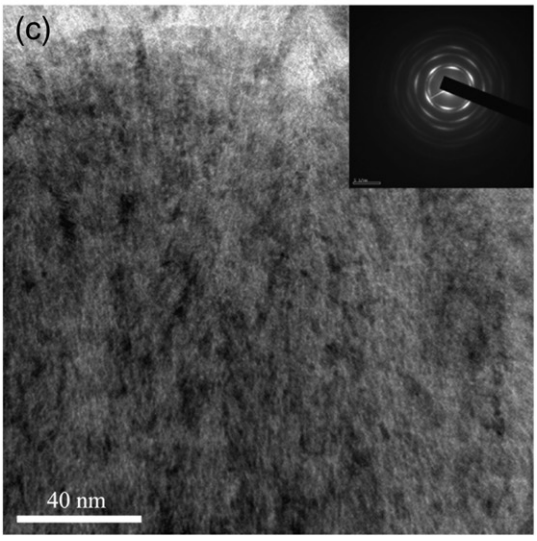

Fig. 2. Cross-view TEM images and SAED patterns obtained from Ti(C, N) layers in the Ti(C, N)/a-C gradient films with different rotation speeds, respectively for (a) 3 rpm (b) 5 rpm and (c) 8 rpm.

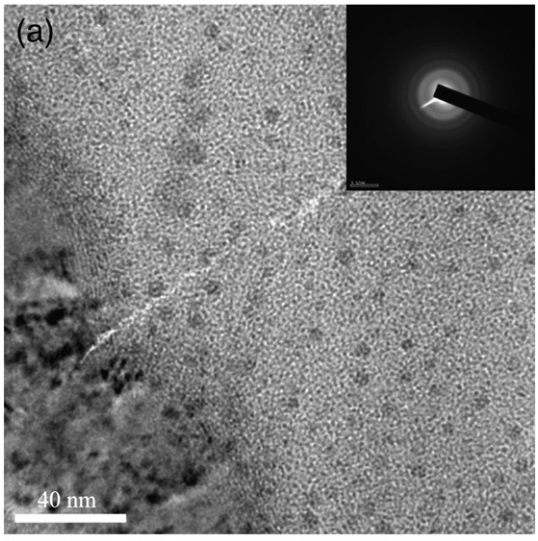

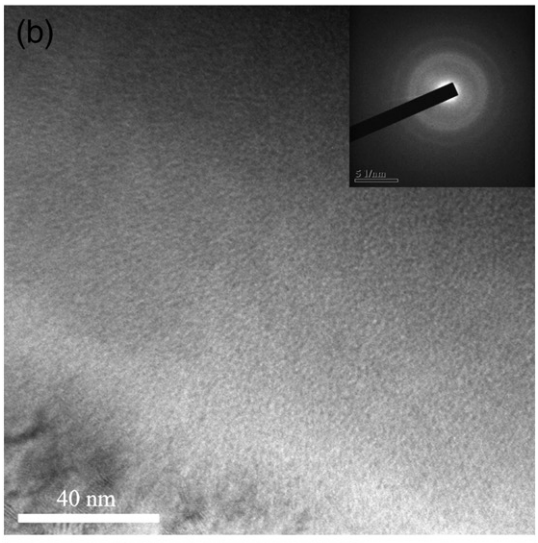

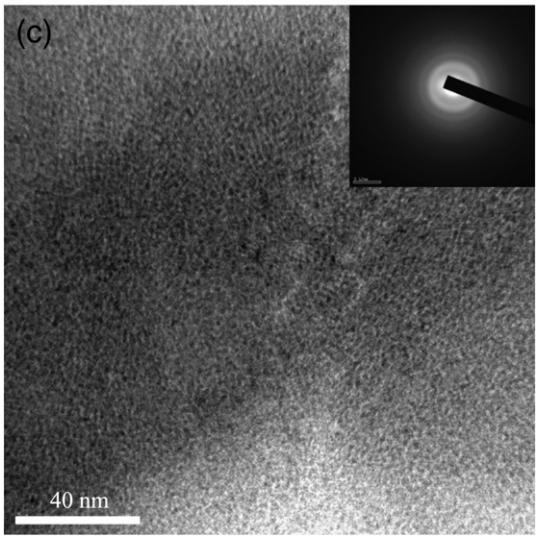

Fig. 3. Cross-view TEM images and SAED patterns obtained from a-C composite layers in the Ti(C, N)/a-C gradient films with different rotation speeds, respectively for (a) 3 rpm (b) 5 rpm and (c) 8 rpm.

the results are not discovered in the other a-C layers that are deposited under 5 and 8 rpm. The appearance of columnar growth is probably due to local ordering of TiC nanograins. In order to investigate the microstructure of surface layers in details, HR-TEM is also employed. The cross-view HR-TEM images of a-C layers as shown in Fig. 4. It is quite evident that the surface a-C layers exhibit typical nanocomposite structure where

the fine TiC nanograins are uniformly embedded in the a-C matrix. The increase in rotation speed not only decreases the size of the nanograins but also leads to the nanograins with more uniform dispersion in the matrix. It is revealed from Fig. 4(a) that the TiC nanograins deposited under the lower speed such as 3 rpm consist of two sizes of 2 nm and 7 nm. But under high rotation speed of 8 rpm, the nanograins have a uniform size of only 2 nm and the dispersed density is also increased. The grains with size below 2 nm are difficult to form in the a-C layer because of the dramatic decrease in the stability of nanograins themselves.

3.2. Mechanical and tribological properties

Fig. 5 shows the microhardness of Ti(C, N)/a-C gradient films varying with the rotation speed of the substrate. The gradient film deposited under the 5 rpm shows a maximum microhardness value of 5310 H_V. The other films show slight low but still high microhardness values, respectively, 4808 H_V of 3 rpm and 4727 H_V of 8 rpm. Generally, the Ti(C, N)/a-C gradient films with a multilayer structure exhibit microhardness higher than the films with no multilayer structure. The decreased period thicknesses in the multilayer structure affect the further microhardness enhancement in the composite films. The composite films showing high microhardness values are mostly driven from Ti(C, N) layers because of their multilayer structure and fine grain size as shown in Fig. 2.

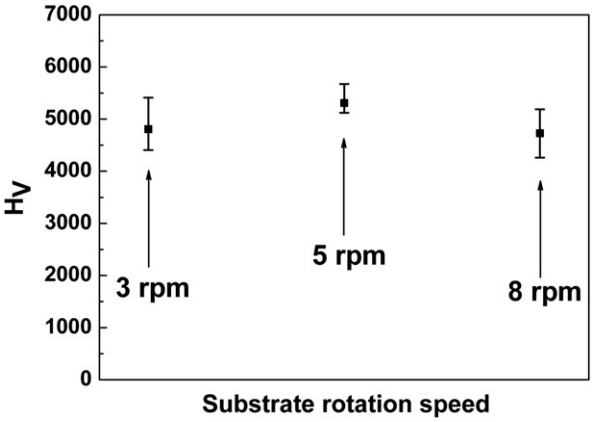

Fig. 5. Microhardness of Ti(C, N)/a-C gradient films.

The friction coefficients of Ti(C, N)/a-C gradient composite films and their specific wear rate are shown in Figs. 6 and 7, respectively. All the gradient films exhibit a rapid decrease from the run-in state to the steady wear state, due to the removal of surface impurities. Generally, the gradient composite films have a friction coefficient below 0.15 and keep the steady low value until the end of friction test. It is noted that the film deposited under 3 rpm shows an obvious fluctuation in the friction coefficient about 0.2 in the steady state, and the ones of others are respectively 0.12 of 5 rpm and 0.15 of 8 rpm show a low and extra steady value. The variations of the friction coefficients in the films deposited under 5 rpm and 8 rpm speeds during the 200 m sliding distance are different. The film under 8 rpm shows slight increased tendency in the friction coefficient but the film under 5 rpm shows steady decrease after sliding for distance of 200 m. This may suggest that the surface a-C layer has been worn out and the substrate Ti(C, N) layer dominates the friction performance of gradient films. The lowest steady friction coefficient is obtained from the film deposited under 5 rpm, which possesses both highest microhardness value and lowest friction coefficient of 0.12. The specific wear rate shown in Fig. 7 also illustrates that the Ti(C, N)/a-C gradient films have excellent wear resistance with the specific wear rates being only 3.7×10^{-17} m^3/mN and 9.7×10^{-17} m^3/mN for the films under 5 rpm and 8 rpm speeds, respectively. Because of comparative thickness values (1.35 μm–1.45 μm), the effect of film thickness on their tribological behavior can be neglected and the thicknesses were respectively measured by SEM and calculated according to the features of the wear traces. It is impossible to calculate the wear rate of film under 3 rpm due to the occurrence of spalling or delamination of the film in friction test.

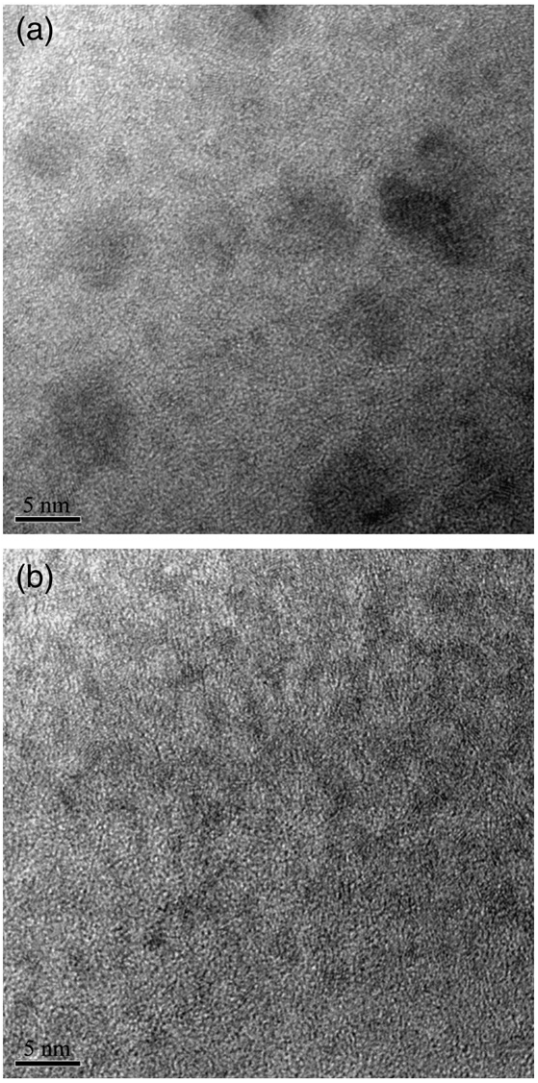

Fig. 4. Cross-view HR-TEM images obtained from a-C layers in the Ti(C, N)/a-C gradient films, respectively for (a) 3 rpm and (b) 8 rpm of rotation speeds.

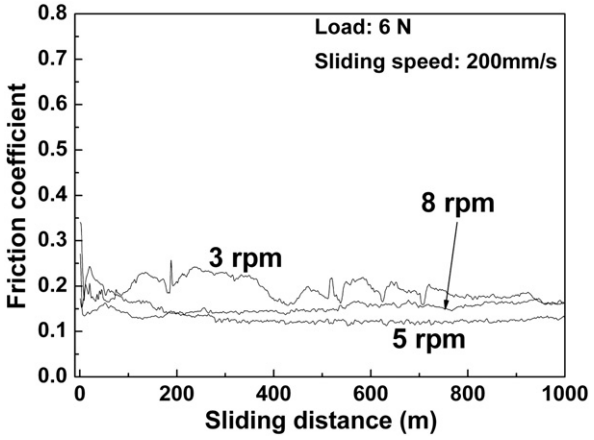

Fig. 6. Friction coefficients of Ti(C, N)/a-C gradient films as a function of sliding distance.

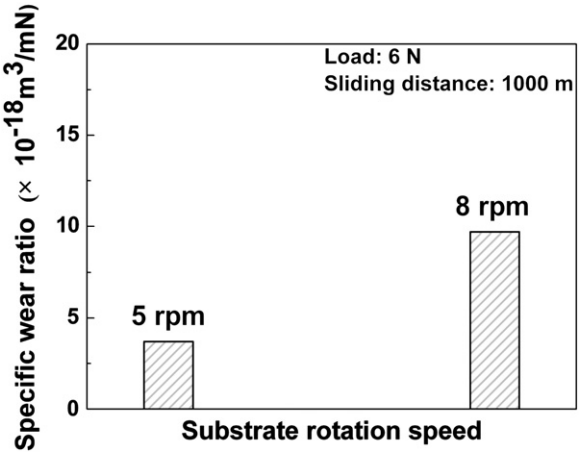

Fig. 7. Specific wear rate of Ti(C, N)/a-C gradient films.

For visible purpose, Fig. 8 shows the morphology of the wear track of Ti(C, N)/a-C gradient composite films.

OM observations of wear tracks reveal that the microcracks initiate and readily propagate to lead to the spalling and delamination of film from the substrate in the film deposited under 3 rpm. From the microstructural observation in Fig. 3(a) and 4(a), the a-C layers in the gradient composite films are found to have TiC nanograins of various sizes (2 nm and 7 nm) distributed in the columnar grains with discontinuous and weak column boundaries. No obvious cracks are observed in the wear tracks on the films under the 5 rpm and the 8 rpm, where the TiC nanograins with uniform size are dispersedly embedded in the a-C matrix in the a-C layer. The surface of the wear tracks is also smooth grinding structure along the sliding direction. The gradient composite film deposited under 5 rpm shows not only low and steady friction coefficients but also low specific wear rates as illustrated in Figs. 6 and 7, respectively.

4. Discussion

Ti(C, N)/a-C gradient composite films exhibit different microstructures from the Ti(C, N) layer to the surface a-C layer, depending on the constituent gradient of the carbon and nitrogen contents. The substrate Ti(C, N) layers show not only a typical columnar growth but also microstructure of a polycrystallite comprising well-crystallized Ti(C, N) crystallites. Following by surface a-C layers which show typical nanocomposite microstructure with TiC nanograins embedded in the amorphous C matrix due to addition of a few titaniums. It is noted that the Ti(C, N) layers also exhibit nano-size multilayer structure which comprises repeated rich-C layer and rich-Ti layer determined by current deposition condition since graphite target chose as the sputtering C supplier. But the result is absent in the a-C layers. Consequently, the rotation speeds affect obviously on the microstructure of composite films. It is clear that the formation and growth of Ti(C, N) columnar grains are restrained by the multilayer structure since the C atoms may decrease the atomic diffusivity on the growing film surface [12], the interrupted effect is obvious when the period thickness of films as well as the repeated rich-C layers are thicker in the deposition of low rotation speed. This is similar to a previous report [13,14]. The grain sizes of the Ti(C, N) layers also gradually decrease accompanied with the microstructure change from the columnar grains to the nanograins as the rotation speed decreases. In the surface a-C layers, the rotation speeds affect obviously on the size and the distribution of TiC nanograins which are finer and more uniformly embedded in the a-C matrix in the high speeds. For magnetron sputtering, the ion bombardment promotes the intermixing of the Ti and C materials to form the nanocomposite structure. It suggests that the frequency of ion bombardment changed by controlling the rotation speeds is also important for the intermixing

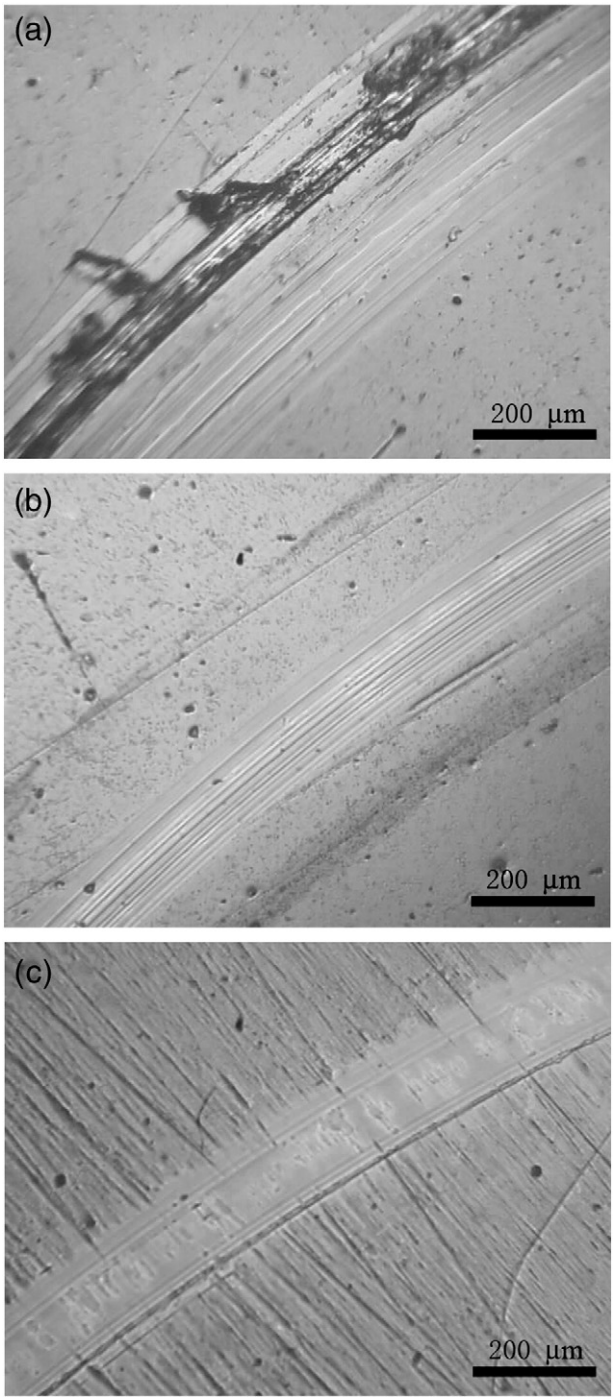

Fig. 8. The OM observations of the wear track obtained from Ti(C, N)/a-C gradient films with different rotation speeds, respectively for (a) 3 rpm (b) 5 rpm and (c) 8 rpm.

of the Ti and C atoms. The microstructure evolution of composite films will result in different performance in the microhardness and friction coefficient of films. Generally, the composite films comprising multilayer Ti(C, N) layers show microhardness higher than that of others. The hardness enhancement by multilayer structure can be explained by Hall–Petch hardening effect and Koehler hardening effect. The latter effect is caused by the difference in the elastic modulus of different layers that limits the propagation of dislocations across layer boundaries [14–16]. The friction properties of films are mainly controlled by the surface a-C layer since the wear initially happened between the a-C layer and the corresponding sliding counterpart. The friction coefficients show a rapid decrease and then keep at almost constant value due to

self-lubrication because of the formation of C-based tribo-layer [17]. The effect of self-lubrication strongly depends on the microstructure of a-C layers. From Fig. 6, the steady and low friction coefficients come from the a-C layers that comprise finer and uniform TiC nanograins. If the size of TiC nanograins is larger and the dispersion of nanograins is inhomogeneously dispersed, the friction properties of the films will be deteriorated obviously because of the spalling or delamination. The large TiC grains may also damage the contact surfaces between the a-C layer and sliding counterpart or the C-based tribo-layer formed. Consequently, the fine and dispersed TiC nanograins can be obtained by increasing the rotation speeds, which not only limit crack initiation crack propagate in the amorphous C matrix but also steady the self-lubrication effect of tribo-layer. Furthermore, the discontinuous and weak columnar boundaries existed in the composite films by low rotation speed discovered from both the Ti(C, N) and the a-C layers may be the origination of crack since the crack initiate and propagate easily through the partial columnar boundaries. It seems that to eliminate the undesired columnar structure by increasing the rotation speeds is important for the composite films.

In general, the gradient composite films comprising hard and lubricant layers by means of a composition gradient can improve the combination properties. The substrate Ti(C, N) layers increase load-carrying capacity of composite films [18,19] and the surface a-C layers provide self-lubrication. According to the results of the mechanical properties and the friction properties, it is clear that the wear rates of the gradient composite films are significantly reduced by the combination of the high microhardness and the low friction coefficient, which can be achieved by controlling the composition gradient and the microstructure in the composite films. The optimized result is obtained from the film deposited under 5 rpm as shown in Fig. 7.

5. Conclusions

Ti(C, N)/a-C gradient films with compositional gradient of films from the substrate to the surface have been prepared by closed-field unbalanced magnetron sputtering ion plating system. The ratio of C to N is controlled by respectively applying the changed power to the graphite target and adjusting the OEM settling point. The prepared Ti(C, N)/a-C composite films have compositional gradient structure which from Ti–TiN-Ti(C, N) to Ti-containing a-C. In the a-C layer, fine TiC nanograins are embedded in a-C matrix. By controlling the rotation speed of substrates, it is possible to prepare the gradient composite films with tailored mechanical properties and tribological properties. The microstructure evolution of composite films suggested that the multilayer structure and good crystallinity of Ti(C, N) combined the surface a-C layer with the fine and uniform dispersion of TiC nanograins which both were important for combination property of the films. The comparing results show that the films deposited by 5 rpm rotation speed have 5310 H_V microhardness value and 0.12 friction coefficient that are higher than 4808 H_V and 4727 H_V and lower than 0.2 and 0.15 of other deposited films by 3 rpm and 8 rpm, respectively. Consequently, the deposited films by 5 rpm also shows excellent wear resistance and have the only wear rate of 3.7×10^{-17} m^3/mN in all films.

Acknowledgments

This work was supported by the National Natural Science Foundation of China (Grant No. 50971097) and the Program for New Century Excellent Talents in University (Grant No. NCET-10-0876).

References

[1] C.H. Wei, J.F. Lin, T.H. Jiang, C.F. Ai, Thin Solid Films 381 (2001) 104.
[2] J. Lin, J.J. Moore, B. Mishra, M. Pinkas, W.D. Sproul, Thin Solid Films 517 (2008) 1131.
[3] T. Zehnder, P. Schwaller, F. Munnik, S. Mikhailov, J. Patscheider, J. Appl. Phys. 95 (2004) 4327.
[4] D. Martinez-Martinez, C. Lopez-Cartes, A. Justo, A. Fernandez, J.C. Sanchez-Lopez, Solid State Sci. 11 (2009) 660.
[5] D. Martinez-Martinez, C. Lopez-Cartes, A. Fernandez, J.C. Sanchez-lopez, Surf. Coat. Technol. 203 (2008) 756.
[6] B. Shi, W.J. Meng, L.E. Rehn, P.M. Baldo, Appl. Phys. Lett. 81 (2002) 352.
[7] Y.T. Pei, D. Galvan, J.Th.M. De Hosson, Acta Mater. 53 (2005) 4505.
[8] J. Musil, Surf. Coat. Technol. 100–101 (1998) 280.
[9] P.J. Kelly, R.D. Arnell, Vacuum 56 (2000) 159.
[10] B. Jonsson, S. Hogmark, Thin Solid Films 114 (1984) 257.
[11] C. Corbella, E. Pascual, G. Oncins, C. Canal, J.L. Andujar, E. Bertran, Thin Solid Films 482 (2005) 293.
[12] X.H. Zhang, J.Q. Jiang, Y.Q. Zeng, J.L. Lin, F.L. Wang, John J. Moore, Surf. Coat. Technol. 203 (2008) 594.
[13] C.Y. Su, C.T. Pan, T.P. Liou, P.T. Chen, C.K. Lin, Surf. Coat. Technol. 203 (2008) 657.
[14] A. Vyas, Y.G. Shen, Z.F. Zhou, K.Y. Li, Compos. Sci. Technol. 68 (2008) 2922.
[15] S. Veprek, J. Vac. Sci. Technol. A 17 (1999) 2401.
[16] P.C. Yashar, W.D. Sproul, Vacuum 55 (1999) 179.
[17] Y.Y. Chang, D.Y. Wang, C.H. Chang, W.T. Wu, Surf. Coat. Technol. 184 (2004) 349.
[18] D.V. Shtansky, T.A. Lobova, V.Yu. Fominski, S.A. Kulinich, I.V. Lyasotsky, M.I. Petrzhik, E.A. Levashov, J.J. Moore, Surf. Coat. Technol. 183 (2004) 328.
[19] H.Y. Ueng, C.T. Guo, Appl. Surf. Sci. 249 (2005) 246.